

Mass-improvement of the vector current in three-flavor QCD

Patrick Fritzsch^a

^a Theoretical Physics Department, CERN, 1211 Geneva 23, Switzerland

Abstract

We determine two improvement coefficients which are relevant to cancel mass-dependent cutoff effects in correlation functions with operator insertions of the non-singlet local QCD vector current. This determination is based on degenerate three-flavor QCD simulations of non-perturbatively $O(a)$ improved Wilson fermions with tree-level improved gauge action. Employing a very robust strategy that has been pioneered in the quenched approximation leads to an accurate estimate of a counterterm cancelling dynamical quark cutoff effects linear in the trace of the quark mass matrix. To our knowledge this is the first time that such an effect has been determined systematically with large significance.

Keywords: Lattice QCD, Nonperturbative Effects, Symanzik improvement
PACS: 11.15.Ha, 11.30.Rd, 12.38.Gc, 12.38.Aw

Contents

1	Prelude	2
2	Centerpiece	3
2.1	Improvement condition of the vector current	3
2.2	Chiral trajectory and current quark mass in finite volume	5
2.3	Unitary quark mass dependence	6
2.4	Valence quark mass dependence	7
2.5	On sea quark mass-effects in the vector channel	9
3	Epilogue	10
	Miscellaneous	11
	References	12

1 Prelude

Lattice QCD has reached a maturity in which some quantities can be computed very precisely such that QED or isospin breaking effects become relevant when compared to experiment. Other quantities are being improved in various ways to match the accuracy reached in state-of-the art experiments, or to use it as input in the search for new physics.

In either case, the control over continuum extrapolations of lattice data is an important ingredient that contributes to the overall precision in any observable. If the QCD action is discretized using Wilson fermions [1], chiral symmetry is broken explicitly by a term proportional to the lattice spacing a , and consequently (renormalized) observables receive contributions linear in the lattice spacing. With some additional effort these terms can be systematically removed as outlined by Symanzik [2–4]. In the present paper we aim at a computation of the coefficients b_V and \bar{b}_V which multiply mass-dependent counterterms to restore a continuum scaling to $O(a^2)$ in the local vector current made of massive quarks. Thus they are relevant in calculations such as semileptonic vector form factors or the muon anomalous magnetic moment.

In cases where the impact of an improvement coefficient seems negligible from a perturbative point of view, it can still be important to have a non-perturbative estimate at hand in order to properly judge at what level of accuracy they will become important. To determine such coefficients one requires well-justified improvement conditions. These conditions can be chosen freely to some extent but differ in complexity and quality regarding statistical and/or systematic effects—like ambiguities at higher order in a . They all remove the leading scaling violation they have been designed for, sometimes at the cost of introducing large contributions at higher orders. The condition explored in the present paper relies on the QCD isospin vector symmetry, and we argue that this method, adopted from reference [5], has little systematic effects. Being implemented in the QCD Schrödinger functional (SF) [6–9] it furthermore allows to efficiently explore the region about the chiral limit over a wide range of couplings and masses at relatively small computational costs. As a result we are able to differentiate between the valence and dynamical (sea) quark sector when the gauge coupling becomes strong.

The pattern of chiral symmetry breaking, inherent to Wilson fermions at finite lattice spacing, intertwines renormalization and $O(a)$ improvement [10]. As a result, the local (isovector) vector current, $V_\mu^a(x) = \bar{\psi}(x)\gamma_\mu\frac{1}{2}\tau^a\psi(x)$, of mass-degenerate fermions renormalizes as¹

$$\begin{aligned}(V_R)_\mu^a &= Z_V(\tilde{g}_0^2) (1 + b_V(g_0^2)am_q + \bar{b}_V(g_0^2) \text{Tr}[aM_q]) (V_I)_\mu^a, \\ (V_I)_\mu^a &= V_\mu^a + c_V(g_0^2)a\tilde{\partial}_\mu T_{\mu\nu}^a,\end{aligned}\tag{1.1}$$

in a *massless renormalization scheme* [5]. Here, V_I is the bare vector current, on-shell $O(a)$ improved through the symmetric lattice derivative of the tensor current $T_{\mu\nu}^a$ with appropriate improvement coefficient c_V . We follow the standard notation in the literature [10, 11] where c_* terms cancel $O(a)$ cutoff effects and b_* , \bar{b}_* the leading mass-dependent effects of order am , induced from the valence or sea quark sector, respectively.² These coefficients are considered functions of the bare gauge coupling g_0^2 while the finite renormalization Z_V has to be evaluated at $\tilde{g}_0^2 = g_0^2(1 + b_g(g_0^2) \text{Tr}[aM_q]/N_f)$ [10, 13, 14] to maintain full $O(a)$ improvement of V_R in the presence of massive quarks. Rather being a mass-dependent finite renormalization than a genuine lattice artefact, the coupling counterterm coefficient $b_g(g_0^2)$ is required to cancel the mass-dependence of g_0^2 in such a way that \tilde{g}_0^2 is mass-independent up to terms of order a^2 . Note that both couplings coincide at the critical line. From eq. (1.1) it then becomes clear that b_V and \bar{b}_V can be determined by individual varying the valence quark mass am_q and sea quark mass $\text{Tr}[aM_q]$.

2 Centerpiece

We are simulating $N_f = 3$ mass-degenerate flavors of Wilson fermions with tree-level improved gauge action in the Schrödinger functional, exhibiting Dirichlet boundary conditions in time and periodic boundary conditions in spatial directions. For on-shell $O(a)$ improvement of the action we use the non-perturbatively determined clover coefficient c_{sw} [15] of ref. [16] and one-loop values of the boundary counterterms c_t and \tilde{c}_t [10, 17, 18]. Except for simulating at non-vanishing quark mass, our setup thus equals the one of ref. [18] with vanishing boundary fields, $T = L$ and $\theta = 1/2$. In the following we adopt the notation of refs. [5, 10, 19].

2.1 Improvement condition of the vector current

For completeness we first introduce the matrix elements used in the present calculation and comment on possible systematic effects. In the SF sources are typically defined on the time boundaries at Euclidean times $x_0 = 0$ and $x_0 = T$,

$$\mathcal{O}^a = a^6 \sum_{\mathbf{u}, \mathbf{v}} \bar{\zeta}(\mathbf{u}) \gamma_5 \frac{1}{2} \tau^a \zeta(\mathbf{v}), \quad \mathcal{O}'^a = a^6 \sum_{\mathbf{u}, \mathbf{v}} \bar{\zeta}'(\mathbf{u}) \gamma_5 \frac{1}{2} \tau^a \zeta'(\mathbf{v}), \tag{2.1}$$

respectively. They are projected to zero momentum and transform according to the vector representation of the exact isospin symmetry. The simplest correlation function is the

¹ Although we are interested in $N_f > 2$ quark flavors, the relevant subgroup for quark bilinears is $SU(2)$.

² In massive schemes it can be convenient to absorb all mass effects into Z -factors and c -coeff., cf. [12].

two-point boundary-to-boundary correlator

$$f_1 = -\frac{1}{3L^6} \langle \mathcal{O}'^a \mathcal{O}^a \rangle \quad (2.2)$$

which up to terms of order a^2 equals the three-point boundary-to-boundary correlator

$$f_{V_R} = \frac{a^3}{6L^6} \sum_{\mathbf{x}} i\epsilon_{abc} \langle \mathcal{O}'^a (V_R)_0^b \mathcal{O}^c \rangle \quad (2.3)$$

with an insertion of the time component of the renormalized vector current, eq. (1.1). It is important to notice that (a) the normalization and improvement of the sources are irrelevant and (b) the $O(a)$ counterterm proportional to c_V cancels as well. Thus two potential sources to $O(a^2)$ ambiguities are absent and the condition becomes

$$f_1 = Z_V (1 + b_V am_q + \bar{b}_V \text{Tr}[aM_q]) f_V(x_0) + O(a^2) \quad (2.4)$$

where f_V as in eq. (2.3) after $(V_R)_0^b \rightarrow V_0^b$ and Z_V the overall normalization in the chiral limit. It also implies that (c) the relation is independent of x_0 up to cutoff effects, or more specifically, independent of c_t and \bar{c}_t . However, if not stated otherwise we take $x_0 = T/2$ as the preferred definition of relation (2.4). Our restricted interest in the mass-improvement coefficients leads to another simplification. Estimators of b_V and \bar{b}_V can be realised as derivatives such that (d) the overall normalization factor Z_V cancels, e.g.,

$$R_V = \frac{\partial}{\partial am_q} \log \left(\frac{f_1}{f_V} \right) \Big|_{m_q=0}, \quad \text{at } M_q = 0 \text{ and } g_0^2 \text{ fixed.} \quad (2.5)$$

The derivative essentially eliminates all mass-independent cutoff effects such that $R_V = b_V + O(am)$ mainly carries ambiguities that depend on the quark mass.³ If the derivative is computed in a range of quark masses where f_1/f_V is dominantly linear, these ambiguities are practically absent as (e) it does not matter at which point the derivative is exactly evaluated. As a consequence of (d)+(e) we conclude that one does not necessarily need to impose a line of constant physics when determining R_V .

Concerning sea quark mass effects we remark that in the unitary case ($m_q = m_{\text{sea}}$) with N_f degenerate quarks ($[M_q]_{ij} = \delta_{ij} m_{\text{sea}}$ with $i, j = 1, \dots, N_f$) only the combination $b_V + N_f \bar{b}_V$ is accessible from eq. (2.4). We thus define

$$\bar{R}_V = \frac{\partial}{\partial am_{\text{sea}}} \log \left(\frac{f_1}{f_V} \right) \Big|_{m_{\text{sea}}=m_q}, \quad \text{at } M_q = 0 \text{ and } g_0^2 \text{ fixed,} \quad (2.6)$$

as estimator for $b_V + N_f \bar{b}_V$ and obtain \bar{b}_V trivially from an appropriate linear combination with R_V . This being said, we proceed as follows: (1) at different values of the lattice spacing we use a given set of dynamical three-flavor simulations with varying sea quark mass to determine the chiral limit ($m_{\text{sea}} = 0$) by simple interpolation, (2) we determine the combination $b_V + N_f \bar{b}_V$ for the unitary case via eq. (2.6), (3) on the ensemble in the vicinity of vanishing quark mass we vary the valence quark masses in order to determine the mass-derivative (2.5) and thus b_V . With above arguments about the potential quality of the improvement conditions (2.5, 2.6), and to keep the numerical effort and costs affordable, we restrict our simulations to lattices of size $L/a = 8$. We show explicitly that this is sufficient in the present case. Our data analysis accounts for autocorrelations via the Γ -method [20] and correlations are included through standard linear error propagation.

³ If the term proportional to c_V would be relevant, it would contribute at $O(am)$ to R_V .

L/a	β	κ_{crit}	\bar{Z}
8	32.0	0.126209(1)	1.020(1)
8	16.0	0.127496(1)	1.033(2)
8	8.0	0.130387(2)	1.073(5)
8	4.0	0.136648(3)	1.226(26)
8	3.7	0.137053(3)	1.283(34)
8	3.6	0.137059(5)	1.318(43)
8	3.5	0.136949(4)	1.414(14)
8	3.4	0.136669(4)	1.566(69)
8	3.3	0.136160(11)	2.02(13)

Table 1: Values of the critical hopping parameters κ_{crit} and slopes \bar{Z} at the unitary point, obtained by linearly interpolating data in the range $|Lm| < 0.22$, see table 2. The resulting uncertainty is combined linearly with the absolute difference to the corresponding values obtained by removing the outermost data points from the least square minimization.

2.2 Chiral trajectory and current quark mass in finite volume

As usual we define the chiral limit as the point where the current quark mass m vanishes.⁴ For simplicity we restrict the discussion to the unitary case ($m_{\text{q}} = m_{\text{sea}}$) and remark that overall (multiplicative) renormalization factors are not required. In the $\mathcal{O}(a)$ improved theory, the relation between current quark mass m and bare subtracted sea quark mass m_{sea} reads

$$m = \bar{Z}m_{\text{sea}}(1 + B am_{\text{sea}}) + \mathcal{O}(a^2) , \quad (2.7)$$

where $\bar{Z} = Zr_{\text{m}}$ is a relative (finite) normalization and B a well-defined combination of mass-improvement coefficients [11]. With similar numerical simulations close to the chiral limit at hand [23], we do apply one iteration of refinements at 9 different values of the gauge coupling $\beta = 6/g_0^2$ to perform simulations in close proximity of $m = 0$. In all cases we are as close as $|am| < 0.001$ and aim for a symmetric variation in the quark mass spanning several orders of magnitude to probe the regime of linearity of eq. (2.7) with significant precision. Where it is possible we go as far as $Lm \approx \pm 2$, but only compile the subset most relevant for the determination of R_{V} and \bar{R}_{V} in table 2, where $am_{\text{sea}} = \frac{1}{2}(\kappa_{\text{sea}}^{-1} - \kappa_{\text{crit}}^{-1})$ is the bare subtracted quark mass based on the critical hopping parameters κ_{crit} of table 1. By steadily increasing the number of points about vanishing current quark mass entering a least square minimisation to a straight line in $1/(2\kappa_{\text{sea}})$, we inspect the quality of the fit to decide on the range of linearity. In all cases, we do not find relevant deviations in the range $|am_{\text{sea}}| < 0.014$. As this is of minor importance anyway, we determine κ_{crit} by fitting to data in that range only. For completeness we give the corresponding slope, \bar{Z} , as estimate for the potential size of Zr_{m} , but have to remind the reader that this quantity is better determined along a line of constant physics. We present a typical interpolation in the top panel of figure 1, compiled from data of table 2 at an intermediate coupling ($\beta = 4.0$) and strong coupling ($\beta = 3.4$). For the latter we know the size of the lattice spacing, $a \approx 0.086$ fm, from ref. [24]. The bare subtracted quark mass at $am_{\text{sea}} = 0.1$ thus corresponds to $m_{\text{sea}} \approx 230$ MeV, and at $am_{\text{sea}} = 0.01$ accordingly to 23 MeV. To state the obvious: within the given uncertainty it is confirmed that the improvement B -term in eq. (2.7) is negligible for up-/down-like quarks while it can be relevant for strange-like quarks, and certainly is for heavier ones.

⁴ We define m as in section A.2.1 of [21] with non-perturbative c_{A} of ref. [22].

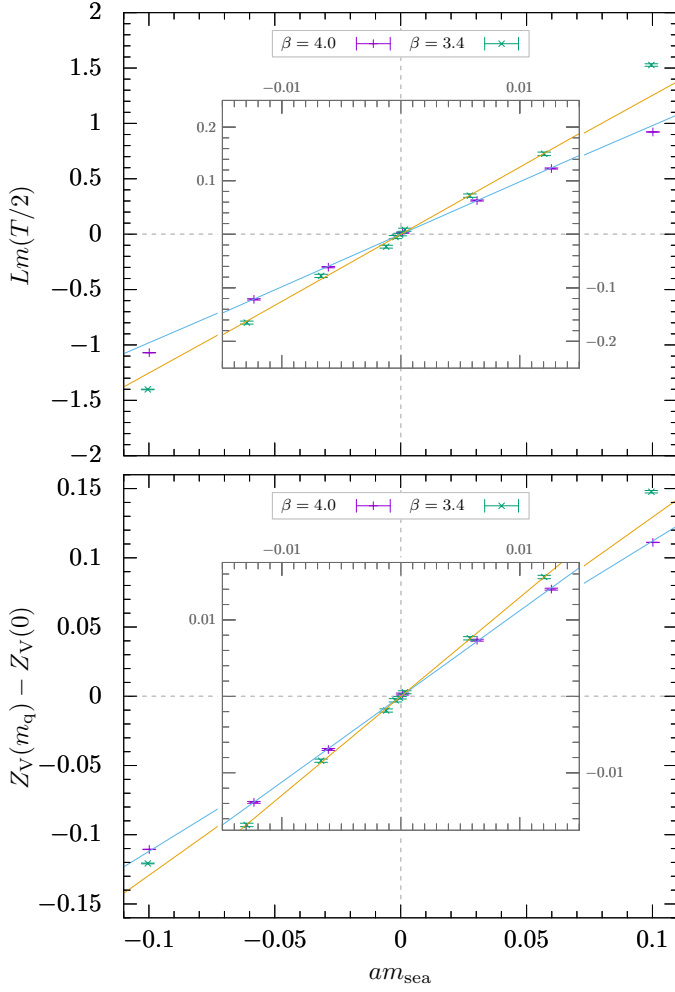


Figure 1: Sea quark mass-dependence ($m_q = m_{\text{sea}}$) of the current quark mass Lm and renormalization factor Z_V with typical interpolating functions at $\beta = 4.0, 3.4$. The inner graph is a magnification of data entering the straight line fit close to the chiral limit ($|am_q| < 0.014$), while the outer graph visualises the deviation from linear behaviour far away from the chiral limit. All data points are independent from each other and taken from table 2. The quality of fit tends to be somewhat better for Z_V data when compared to Lm data. Note that the fit quality of Lm at $\beta = 3.4$ improves when the points atop $|am_q| = 0.012$ are included.

2.3 Unitary quark mass dependence

We have measured the correlation functions f_1 and f_V in the unitary setup for all sea quark masses. Their values are listed in table 2 in dependence of m_{sea} and we use $Z_V(m_q)$ as short hand for the mass-dependent ratio $f_1(m_q)/f_V(m_q)$. We clearly profit from correlations between the two boundary-to-boundary correlation functions but note that values on different ensembles are uncorrelated. As in the previous section we study the range in which the data is well compatible with a straight line fit ansatz, which again is the case for $|am_{\text{sea}}| < 0.014$, cf. bottom panel of figure 1. At each coupling β we neglect the ensemble closest to the chiral limit in order to be fully independent from the determination of R_V presented in the next section. The associated interpolation provides the intercept at $m_{\text{sea}} = 0$ and mass-derivative $\partial_{m_q} Z_V(m_q)$. Combined they give estimates of \bar{R}_V as listed in table 3. Its uncertainty is about one percent and below. For reasons described in the next section, we increase the uncertainty of \bar{R}_V at $\beta = 3.3$ before probing various trial

Padé functions in a weighted least square minimisation. The data is best described by

$$\bar{R}_V(g_0^2) = \frac{1 + \bar{p}_1 g_0^2 + \bar{p}_2 g_0^4 + \bar{p}_3 g_0^6}{1 + \bar{p}_4 g_0^2}, \quad (\bar{p}_i) = \begin{pmatrix} -0.43101 \\ +0.04109 \\ -0.03911 \\ -0.51771 \end{pmatrix}, \quad (2.8)$$

which we take as our preferred representation of $b_V + N_f \bar{b}_V$. With the accuracy achieved in the present paper, its uncertainty is not really of any practical relevance, except when we derive the uncertainty of \bar{b}_V in section 2.5. For completeness we quote $(i, j = 1, \dots, 4)$

$$\text{cov}(\bar{p}_i, \bar{p}_j) = \begin{pmatrix} 4.9676 & -4.8982 & 3.0473 & 3.2513 \\ * & 6.4514 & -3.6515 & -2.6826 \\ * & * & 2.1830 & 1.8785 \\ * & * & * & 2.4558 \end{pmatrix} \times 10^{-5}. \quad (2.9)$$

The functional form (2.8) is plotted in figure 3 together with the input data. We should remark that the improvement coefficient b_V is known to one-loop order in perturbation theory [9, 25], $b_V^{\text{PT}}(g_0^2) = 1 + 0.0886(2)C_F g_0^2 = 1 + 0.1181(3)g_0^2$. As the leading contribution of \bar{b}_V is at $O(g_0^4)$, we could constrain all Padé ansätze by $b_V^{\text{PT}}(g_0^2)$. However, the accuracy of our data, especially at small couplings ($\beta = 32.0, 16.0$), reveals some tension to the one-loop estimate which is hard to account for in that case: $\bar{p}_1 - \bar{p}_4 = 0.087(3)$. This could be due to the asymptotic nature of the perturbative series when compared to a non-perturbative result, or may expose a point we have not stressed explicitly yet. We have argued that the normalization conditions in use have hardly any systematic effects. On the other hand they explicitly depend on the non-perturbative clover-coefficient c_{sw} [16] that renders the Wilson action $O(a)$ improved. Although the Padé ansatz used for $c_{\text{sw}}(g_0^2)$ accounts for the correct one-loop coefficient, it undershoots it at couplings below $g_0^2 \approx 0.9$ and approaches it only asymptotically. In that respect it is similar to what we observe but without data in the deep perturbative regime.

Of course, this would have gone unnoticed as any fit excluding our $\beta = 32.0, 16.0$ data can be easily constrained by the aforementioned one-loop b_V^{PT} . In the end, this discussion is of purely academic interest as no simulation of physical interest is ever performed in that region of couplings. But it is the reason why we do not insist in constraining our final result, eq. (2.8).

2.4 Valence quark mass dependence

Next we come to our determination of b_V which is required in a partially quenched setup, e.g., with charmed valence quarks. For that purpose, we choose the ensemble closest to vanishing quark mass at each coupling, and for convenience measure f_1 and f_V with hopping parameters κ_{val} coinciding with the κ_{sea} of other simulations listed in table 2. As a result, the measurements of $Z_V(m_q)$ for different valence quark masses are strongly correlated, leading to much more accurate estimates of R_V . Even with higher accuracy, we do not observe mentionable differences from linearity in the range $|am_q| < 0.014$ and as in the previous section stick to it in our final analysis. Before continuing we want to present a stringent test to explicitly validate the use of $L/a = 8$ lattices.

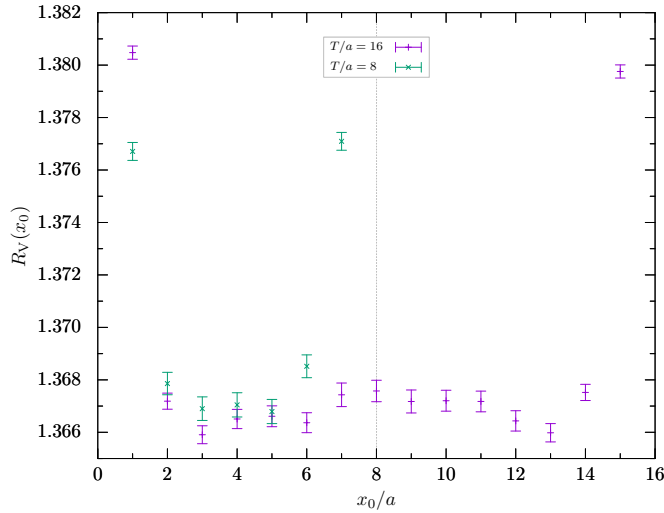


Figure 2: Euclidean time (in)dependence of R_V at $\beta = 4.0$ for $L/a = 8, 16$ lattices. Straight line interpolations take all correlations into account for the data shown here. Except for the points closest to the boundaries, there is no statistically significant x_0 -dependence.

In figure 2 we show the Euclidean time dependence of R_V at $\beta = 4.0$ where two volumes are at our disposal, $T = L = 8a, 16a$. The latter is available to us thanks to the work in ref. [18, 26], and we refer to it for further details about that simulation. First, it confirms that, one or two lattice units away from the boundaries, there is no x_0 -dependence beyond statistical fluctuations, suggesting that $O(a^2)$ effects in eq. (2.4) are small. Second, the agreement of $R_V(T/2)$ between both volumes shows that our estimate is volume independent. These observations hold within the statistical uncertainty which is at the per mille level or below. Monitoring the x_0 -dependence for all values of β , we remark that only at the coarsest lattice spacing ($\beta = 3.3$) we observe a $+2\sigma$ deviation in both $R_V(T/2 + a)$ and $R_V(T/2 - a)$. To account for this still insignificant fluctuation, we conservatively double the uncertainty of $R_V(T/2)$.

We compile results of R_V for two types of analysis in table 3. For reasons that become clear soon, we distinguish between a full (correlated) analysis and one neglecting correlations between measurements at different masses, which increases the uncertainty of R_V by about an order of magnitude. Of course, both are in full agreement. In the course of simulations to produce ensembles at different sea quark masses we were guided by the statistical precision in \bar{R}_V , leading to a precision in the correlated analysis of R_V that goes far beyond what is needed in future applications. While it allowed to probe relation (2.4) and the range of linearity more precisely than before, it is not straightforward to find a proper global approximation at that level of precision without increasing the number of data points.

For the sake of simplicity we thus prefer to employ data from the uncorrelated analysis on each ensemble, remarking once more that results at different couplings are statistically independent. At $\beta = 4.0$ we furthermore include the independent data point from $L/a = 16$. Not surprisingly, a $[3, 1]$ -Padé function gives the best result that reads

$$R_V(g_0^2) = \frac{1 + p_1 g_0^2 + p_2 g_0^4 + p_3 g_0^6}{1 + p_4 g_0^2}, \quad (p_i) = \begin{pmatrix} -0.40040 \\ +0.04352 \\ -0.03852 \\ -0.48803 \end{pmatrix}, \quad (2.10)$$

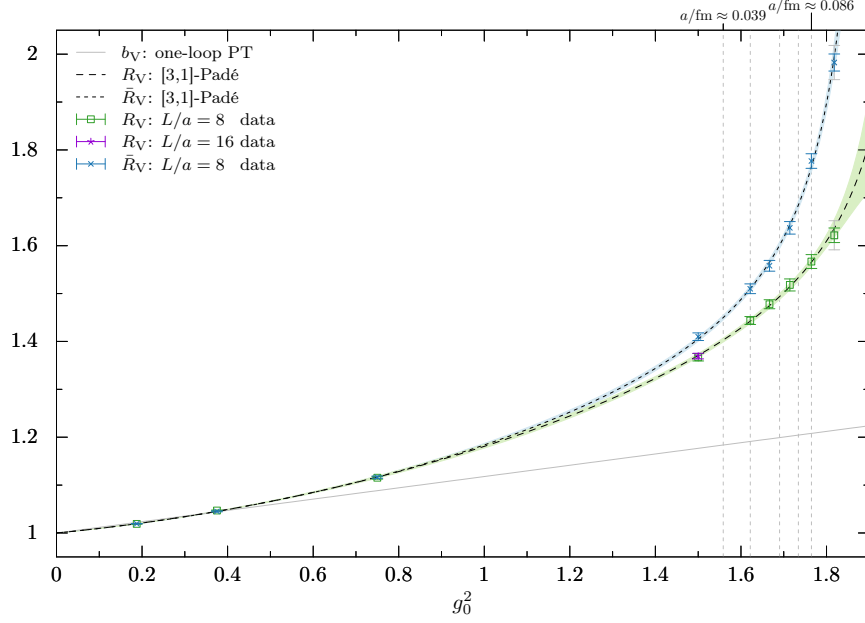


Figure 3: Data with interpolating function for R_V and \bar{R}_V in comparison to the known perturbative one-loop estimate b_V^{PT} , see text. Vertical dashed lines mark values of $\beta \in \{3.4, 3.46, 3.55, 3.7, 3.85\}$ used in large volume simulations [24, 27, 28], with indicated largest and smallest lattice spacing a .

with parameter covariance matrix

$$\text{cov}(p_i, p_j) = \begin{pmatrix} 86.1424 & -20.5770 & 23.7151 & 78.9559 \\ * & 8.1121 & -6.9724 & -17.7160 \\ * & * & 7.1199 & 21.3673 \\ * & * & * & 72.9602 \end{pmatrix} \times 10^{-5}. \quad (2.11)$$

We add this interpolation and the entering data points to figure 3. One observes a significant difference to \bar{R}_V in the strong coupling region where (2+1)-flavor large volume simulations with the same bulk lattice action, produced by the Coordinated Lattice Simulations effort (CLS), exist [24, 27, 29]. Based on those simulations various estimates of mass-improvement coefficients have been published in ref. [30] for $\beta \in \{3.4, 3.46, 3.55, 3.7\}$. The uncertainty of the latter for b_V is of the size of our estimated difference between sea and valence quark sector.

2.5 On sea quark mass-effects in the vector channel

With interpolating formulae for R_V and \bar{R}_V we are finally able to check on the size of pure sea quark mass-effects that are cancelled at leading order by the counterterm $\bar{b}_V \text{Tr}[aM_q]$. We define

$$\bar{b}_V(g_0^2) = (\bar{R}_V(g_0^2) - R_V(g_0^2)) / N_f \quad (2.12)$$

by eq. (2.8, 2.10) and present it in figure 4. \bar{R}_V and R_V are statistically independent, such that the uncertainty of \bar{b}_V follows trivially from standard Gaussian error propagation. The value of \bar{b}_V is different from zero in the non-perturbative region of large volume simulations [27], being about 0.07 at $\beta = 3.4$. For those simulations the unsubtracted trace of the

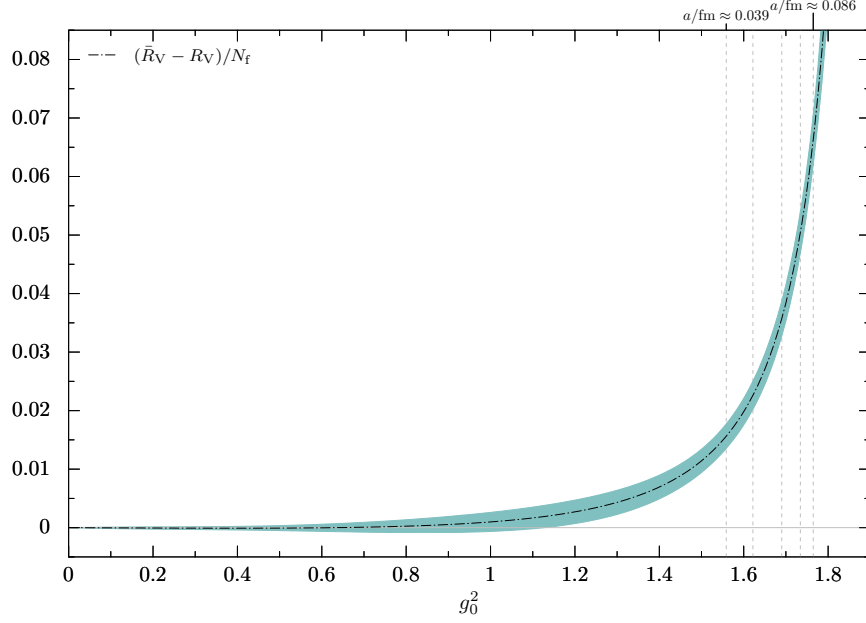


Figure 4: Sea quark mass-improvement coefficient $\bar{b}_V = (\bar{R}_V - R_V)/N_f$.

quark mass matrix has been kept constant w.r.t. the $SU(3)$ -flavor symmetric point such that the physics at fixed coupling g_0^2 and $\text{Tr}[aM_q]$, and thus fixed \tilde{g}_0^2 , does not require any knowledge of b_g . With $\sum_{i=u,d,s} (2\kappa_i)^{-1} \approx 10.97$ at $\beta = 3.4$ and an preliminary estimate $\kappa_{\text{crit}}(\beta) \approx 0.13698$ of ref. [23] this implies $\text{Tr}[aM_q] \approx 0.02$. The resulting counterterm to cancel mass-dependent sea quark cutoff effects of a strange quark thus becomes an effect at the per mille level. For a dynamical heavy charm quark in the sea this effect would rise to the per cent level even without including higher order effects.

Given the similarity between b_A , b_P and b_V , cf. [14], one could be lead to the assumption that \bar{b}_A and \bar{b}_P are comparable in size to the result for \bar{b}_V presented above, but only a direct computation can confirm that.

3 Epilogue

In combination with a precise determination of the overall renormalization factor Z_V and improvement coefficient c_V along a line of constant physics [31–33], the determination of \bar{b}_V and b_V presented in this paper completes the on-shell $O(a)$ improvement of the non-singlet local vector current with massive Wilson fermions that is consistent with massless renormalization schemes. Our results are independent from determinations of Z_V and c_V , and thanks to the applied improvement conditions we have reached very accurate estimates of \bar{R}_V and R_V that allowed for disentangling sea and valence quark effects with large significance for the first time. These estimates are particularly relevant to lattice phenomenology on CLS (2+1)-flavor ensembles with lattice spacings in the range $0.04 \lesssim a/\text{fm} \lesssim 0.09$. Due to the smallness of \bar{b}_V even at the non-perturbative level ($a \lesssim 0.1 \text{ fm}$) it seems likely that these effects are negligible in most applications of lattice QCD with dynamical light quarks. We have shown explicitly that higher order mass-dependent effects are practically absent, which is not true anymore for, e.g., dynamical charm quarks.

Acknowledgements. We thank M. Lüscher for a critical reading of the manuscript. P.F. acknowledges financial support by the Spanish MINECO’s “Centro de Excelencia Severo Ochoa” Programme under grant SEV-2012-0249, as well as from the MCINN grant FPA2012-31686. The main part of this work has profited from the IFT computing infrastructure, especially the Hydra cluster, and some additional measurements were performed on the CERN cluster. We thank both IT departments for the provided resources and support.

Miscellaneous

Let there be table 2 and 3.

Table 2: Unitary simulation points with corresponding current quark mass and correlator results. After thermalization, the majority of simulations has accumulated ensemble sizes of 5000 configurations or more, separated by 4 molecular dynamic units each. Measurements have been performed on each configuration.

β	κ_{sea}	am_{sea}	Lm	$f_1(m_q)$	$f_V(m_q) _{x_0=T/2}$	$Z_V(m_q)$
32	0.12581342	+0.0125	+0.101367(54)	1.23284(22)	1.23354(22)	0.999436(9)
	0.12601159	+0.0062	+0.050765(52)	1.32366(28)	1.33279(29)	0.993145(9)
	0.12621039	−0.0000	+0.000059(53)	1.42134(29)	1.44025(30)	0.986870(9)
	0.12640982	−0.0063	−0.051145(55)	1.52593(33)	1.55616(34)	0.980575(9)
	0.12660988	−0.0125	−0.102681(55)	1.63694(33)	1.68015(35)	0.974285(9)
16	0.12709186	+0.0125	+0.10271(12)	1.11557(45)	1.13923(47)	0.979236(18)
	0.12729408	+0.0062	+0.05158(13)	1.20192(49)	1.23538(51)	0.972914(17)
	0.12749695	−0.0000	+0.00006(12)	1.29321(56)	1.33789(60)	0.966599(20)
	0.12770047	−0.0063	−0.05186(12)	1.39299(60)	1.45057(64)	0.960303(18)
	0.12790464	−0.0125	−0.10388(12)	1.49863(69)	1.57094(75)	0.953969(19)
8	0.12996592	+0.0124	+0.10633(29)	0.89988(96)	0.9641(10)	0.933404(42)
	0.13017740	+0.0062	+0.05294(30)	0.9772(10)	1.0541(11)	0.926998(43)
	0.13038957	−0.0001	+0.00002(29)	1.0566(11)	1.1477(12)	0.920627(40)
	0.13060244	−0.0063	−0.05432(36)	1.1459(15)	1.2535(16)	0.914155(53)
	0.13060244	−0.0063	−0.05348(45)	1.1477(19)	1.2555(21)	0.914138(58)
	0.13081600	−0.0126	−0.10846(29)	1.2468(14)	1.3735(16)	0.907710(40)
4	0.13300823	+0.1007	+0.9229(11)	0.1059(4)	0.1169(4)	0.90578(12)
	0.13617797	+0.0132	+0.1228(11)	0.5150(21)	0.6369(26)	0.80868(12)
	0.13641017	+0.0070	+0.0631(11)	0.5735(25)	0.7151(32)	0.80201(13)
	0.13664316	+0.0007	+0.0028(11)	0.6462(28)	0.8129(35)	0.79497(12)
	0.13687696	−0.0055	−0.0615(12)	0.7339(32)	0.9316(42)	0.78773(13)
	0.13711155	−0.0118	−0.1216(12)	0.8106(37)	1.0381(48)	0.78080(12)
	0.14048236	−0.0993	−1.0699(14)	3.270(37)	4.781(55)	0.68408(14)
3.7	0.13659066	+0.0124	+0.1264(15)	0.4593(21)	0.5876(27)	0.78168(14)
	0.13682427	+0.0061	+0.0625(14)	0.5245(25)	0.6774(33)	0.77429(15)
	0.13702933	+0.0007	+0.0063(16)	0.5929(34)	0.7721(45)	0.76794(16)
	0.13705868	−0.0001	+0.0002(15)	0.5984(35)	0.7800(46)	0.76723(17)
	0.13705868	−0.0001	−0.0021(13)	0.5983(24)	0.7799(32)	0.76719(12)
	0.13708804	−0.0009	−0.0096(15)	0.6156(32)	0.8035(43)	0.76606(15)
	0.13729390	−0.0064	−0.0632(15)	0.6815(42)	0.8966(56)	0.76015(15)
	0.13752992	−0.0126	−0.1318(16)	0.7791(46)	1.0353(62)	0.75254(17)
3.6	0.13659365	+0.0125	+0.1303(18)	0.4466(26)	0.5797(35)	0.77043(17)

	0.13682727	+0.0062	+0.0650(18)	0.5149(29)	0.6746(39)	0.76326(16)
	0.13703235	+0.0008	+0.0075(19)	0.5844(35)	0.7723(47)	0.75668(17)
	0.13706169	-0.0000	-0.0011(15)	0.5876(28)	0.7775(37)	0.75574(14)
	0.13709105	-0.0008	-0.0076(18)	0.6004(36)	0.7950(48)	0.75514(18)
	0.13729692	-0.0063	-0.0639(18)	0.6781(42)	0.9060(56)	0.74848(16)
	0.13753296	-0.0125	-0.1348(17)	0.7799(48)	1.0525(66)	0.74100(17)
3.5	0.13647158	+0.0127	+0.1448(21)	0.4202(28)	0.5539(37)	0.75864(18)
	0.13670478	+0.0065	+0.0726(24)	0.4980(37)	0.6631(50)	0.75107(21)
	0.13693878	+0.0002	+0.0038(22)	0.5721(41)	0.7698(55)	0.74310(17)
	0.13717359	-0.0060	-0.0687(23)	0.6770(47)	0.9203(65)	0.73562(20)
	0.13740920	-0.0123	-0.1380(22)	0.7883(59)	1.0823(82)	0.72836(20)
3.4	0.13304903	+0.0996	+1.527(11)	0.0077(4)	0.0088(4)	0.87560(87)
	0.13622073	+0.0121	+0.1502(33)	0.4129(43)	0.5554(59)	0.74346(22)
	0.13645308	+0.0058	+0.0721(32)	0.4990(44)	0.6785(60)	0.73544(21)
	0.13665703	+0.0003	+0.0085(29)	0.5804(50)	0.7969(69)	0.72839(19)
	0.13667180	-0.0001	-0.0005(24)	0.5896(35)	0.8102(49)	0.72767(16)
	0.13668622	-0.0004	-0.0052(30)	0.5934(53)	0.8158(74)	0.72734(22)
	0.13671542	-0.0012	-0.0233(30)	0.6138(50)	0.8454(70)	0.72601(21)
	0.13692016	-0.0067	-0.0777(31)	0.7066(55)	0.9822(78)	0.71944(21)
	0.13715490	-0.0129	-0.1649(28)	0.8364(74)	1.176(10)	0.71105(22)
	0.14052786	-0.1004	-1.4014(30)	3.12(60)	5.139(99)	0.60712(29)
3.3	0.13573478	+0.0114	+0.1933(65)	0.3815(71)	0.525(10)	0.72595(24)
	0.13596547	+0.0051	+0.0870(58)	0.5073(72)	0.708(10)	0.71697(23)
	0.13613900	+0.0005	+0.0068(46)	0.6076(63)	0.8558(89)	0.70995(22)
	0.13619695	-0.0011	-0.0225(42)	0.6539(64)	0.9242(92)	0.70761(23)
	0.13625494	-0.0027	-0.0444(41)	0.6875(75)	0.974(11)	0.70555(21)
	0.13642921	-0.0074	-0.1052(52)	0.7913(98)	1.131(14)	0.69959(27)
	0.13666227	-0.0136	-0.2181(47)	0.988(11)	1.431(15)	0.69083(27)

References

- [1] K. G. Wilson, *Confinement of Quarks*, *Phys.Rev.* **D10** (1974) 2445–2459.
- [2] K. Symanzik, *Continuum Limit and Improved Action in Lattice Theories. 1. Principles and ϕ^4 theory*, *Nucl.Phys.* **B226** (1983) 187.
- [3] K. Symanzik, *Continuum Limit and Improved Action in Lattice Theories. 2. $O(N)$ nonlinear sigma model in perturbation theory*, *Nucl.Phys.* **B226** (1983) 205.
- [4] K. Symanzik, *Some Topics in Quantum Field Theory*, in *Mathematical Problems in Theoretical Physics. Proceedings, 6th International Conference on Mathematical Physics, West Berlin, Germany, August 11-20, 1981*, pp. 47–58, 1981.
[doi:10.1007/3-540-11192-1_11].
- [5] M. Lüscher, S. Sint, R. Sommer and H. Wittig, *Nonperturbative determination of the axial current normalization constant in $O(a)$ improved lattice QCD*, *Nucl.Phys.* **B491** (1997) 344–364, [hep-lat/9611015].
- [6] M. Lüscher, R. Narayanan, P. Weisz and U. Wolff, *The Schrödinger functional: A Renormalizable probe for non-Abelian gauge theories*, *Nucl.Phys.* **B384** (1992) 168–228, [hep-lat/9207009].

Table 3: Summary of results and data analysis for \bar{R}_V and R_V , using input data in the range $|am_q| < 0.014$. Note that the simulation of $L/a = 16$ at $\beta = 4.0$ has $\kappa = 0.13668396$ and $Lm = 0.0006(8)$, cf. table 10 of ref. [26]. (top rows: uncorrelated analysis, bottom rows: fully correlated analysis)

L/a	β	sea sector			valence sector		
		$Z_V(0)$	$\partial_m Z_V$	\bar{R}_V	$Z_V(0)$	$\partial_m Z_V$	R_V
8	32	0.986902(4)	1.0059(5)	1.0193(5)	0.986909(4)	1.0057(5)	1.0190(5)
8	16	0.966639(8)	1.0103(10)	1.0452(10)	0.966633(9)	1.0119(10)	1.0469(10)
8	8	0.920652(18)	1.0279(21)	1.1165(22)	0.920647(24)	1.0269(27)	1.1154(29)
8	4	0.794704(56)	1.1205(63)	1.4099(79)	0.794802(54)	1.0865(62)	1.3670(77)
16	4	—	—	—	0.786608(20)	1.0772(46)	1.3694(58)
8	3.7	0.767303(54)	1.1586(78)	1.510(10)	0.767307(47)	1.1078(63)	1.4437(82)
8	3.6	0.755889(62)	1.1777(85)	1.558(11)	0.755754(53)	1.1168(71)	1.4777(94)
8	3.5	0.743022(85)	1.2165(97)	1.637(13)	0.742886(83)	1.1277(94)	1.518(13)
8	3.4	0.727888(72)	1.293(11)	1.777(15)	0.727381(73)	1.140(10)	1.567(14)
8	3.3	0.709415(89)	1.406(13)	1.983(18)	0.708629(81)	1.149(11)	1.622(15)
8	32	—	—	—	0.98691(1)	1.00566(2)	1.01900(2)
8	16	—	—	—	0.96663(2)	1.01195(3)	1.04688(4)
8	8	—	—	—	0.92065(5)	1.02686(9)	1.1154(1)
8	4	—	—	—	0.79480(12)	1.0865(3)	1.3670(5)
16	4	—	—	—	0.78762(5)	1.0771(3)	1.3676(4)
8	3.7	—	—	—	0.76731(13)	1.1078(4)	1.4437(6)
8	3.6	—	—	—	0.75575(14)	1.1167(5)	1.4777(7)
8	3.5	—	—	—	0.74289(18)	1.1277(7)	1.5181(10)
8	3.4	—	—	—	0.72738(20)	1.1405(8)	1.5679(14)
8	3.3	—	—	—	0.70864(21)	1.1516(9)	1.6251(15)

- [7] S. Sint, *On the Schrödinger functional in QCD*, *Nucl.Phys.* **B421** (1994) 135–158, [[hep-lat/9312079](#)].
- [8] M. Lüscher and P. Weisz, *On-Shell Improved Lattice Gauge Theories*, *Commun.Math.Phys.* **97** (1985) 59, [Erratum-ibid. **98** (1985) 433].
- [9] S. Aoki, R. Frezzotti and P. Weisz, *Computation of the improvement coefficient c_{SW} to one loop with improved gluon actions*, *Nucl.Phys.* **B540** (1999) 501–519, [[hep-lat/9808007](#)].
- [10] M. Lüscher, S. Sint, R. Sommer and P. Weisz, *Chiral symmetry and $O(a)$ improvement in lattice QCD*, *Nucl.Phys.* **B478** (1996) 365–400, [[hep-lat/9605038](#)].
- [11] T. Bhattacharya, R. Gupta, W. Lee, S. R. Sharpe and J. M. Wu, *Improved bilinears in lattice QCD with non-degenerate quarks*, *Phys.Rev.* **D73** (2006) 034504, [[hep-lat/0511014](#)].
- [12] P. Fritzsch, R. Sommer, F. Stollenwerk and U. Wolff, *Symanzik Improvement with Dynamical Charm: A 3+1 Scheme for Wilson Quarks*, **1805.01661**.
- [13] S. Sint and R. Sommer, *The running coupling from the QCD Schrödinger functional: a one-loop analysis*, *Nucl.Phys.* **B465** (1996) 71–98, [[hep-lat/9508012](#)].
- [14] S. Sint and P. Weisz, *Further results on $O(a)$ improved lattice QCD to one-loop order of perturbation theory*, *Nucl.Phys.* **B502** (1997) 251–268, [[hep-lat/9704001](#)].
- [15] B. Sheikholeslami and R. Wohlert, *Improved Continuum Limit Lattice Action for QCD with Wilson Fermions*, *Nucl.Phys.* **B259** (1985) 572.

- [16] J. Bulava and S. Schaefer, *Improvement of $N_f = 3$ lattice QCD with Wilson fermions and tree-level improved gauge action*, *Nucl.Phys.* **B874** (2013) 188–197, [[1304.7093](#)].
- [17] S. Takeda, S. Aoki and K. Ide, *A Perturbative determination of $O(a)$ boundary improvement coefficients for the Schrödinger functional coupling at one loop with improved gauge actions*, *Phys.Rev.* **D68** (2003) 014505, [[hep-lat/0304013](#)].
- [18] ALPHA COLLABORATION, M. Dalla Brida, P. Fritzsche, T. Korzec, A. Ramos, S. Sint and R. Sommer, *Slow running of the Gradient Flow coupling from 200 MeV to 4 GeV in $N_f = 3$ QCD*, *Phys. Rev.* **D95** (2017) 014507, [[1607.06423](#)].
- [19] R. Hoffmann, *Chiral properties of dynamical Wilson fermions*. PhD thesis, Humboldt-Universität zu Berlin, Mathematisch-Naturwissenschaftliche Fakultät I, 2005. [[hep-lat/0510119](#)]. [[doi:10.18452/15341](#)].
- [20] ALPHA COLLABORATION, U. Wolff, *Monte Carlo errors with less errors*, *Comput.Phys.Commun.* **156** (2004) 143–153, [[hep-lat/0306017](#)], [Erratum-ibid. **176** (2007) 383].
- [21] ALPHA COLLABORATION, S. Capitani, M. Lüscher, R. Sommer and H. Wittig, *Nonperturbative quark mass renormalization in quenched lattice QCD*, *Nucl.Phys.* **B544** (1999) 669–698, [[hep-lat/9810063](#)], [Erratum-ibid. **B582** (2000) 762–762].
- [22] ALPHA COLLABORATION, J. Bulava, M. Della Morte, J. Heitger and C. Wittemeier, *Non-perturbative improvement of the axial current in $N_f = 3$ lattice QCD with Wilson fermions and tree-level improved gauge action*, *Nucl.Phys.* **B896** (2015) 555–568, [[1502.04999](#)].
- [23] P. Fritzsche and T. Korzec, “Simulating the QCD Schrödinger Functional with three massless quark flavors.” in preparation.
- [24] M. Bruno, T. Korzec and S. Schaefer, *Setting the scale for the CLS 2 + 1 flavor ensembles*, *Phys. Rev.* **D95** (2017) 074504, [[1608.08900](#)].
- [25] Y. Taniguchi and A. Ukawa, *Perturbative calculation of improvement coefficients to $O(g^2a)$ for bilinear quark operators in lattice QCD*, *Phys.Rev.* **D58** (1998) 114503, [[hep-lat/9806015](#)].
- [26] ALPHA COLLABORATION, I. Campos, P. Fritzsche, C. Pena, D. Preti, A. Ramos and A. Vladikas, *Non-perturbative quark mass renormalisation and running in $N_f = 3$ QCD*, *Eur. Phys. J.* **C78** (2018) 387, [[1802.05243](#)].
- [27] M. Bruno, D. Djukanovic, G. P. Engel, A. Francis, G. Herdoíza et al., *Simulation of QCD with $N_f = 2 + 1$ flavors of non-perturbatively improved Wilson fermions*, *JHEP* **1502** (2015) 043, [[1411.3982](#)].
- [28] ALPHA COLLABORATION, M. Bruno, M. Dalla Brida, P. Fritzsche, T. Korzec, A. Ramos, S. Schaefer et al., *QCD Coupling from a Nonperturbative Determination of the Three-Flavor Λ Parameter*, *Phys. Rev. Lett.* **119** (2017) 102001, [[1706.03821](#)].
- [29] D. Mohler, S. Schaefer and J. Simeth, *CLS 2+1 flavor simulations at physical light- and strange-quark masses*, in *Proceedings, 35th International Symposium on Lattice Field Theory (Lattice 2017): Granada, Spain, June 18–24, 2017*, vol. 175, p. 02010, 2018. [[1712.04884](#)]. [[doi:10.1051/epjconf/201817502010](#)].
- [30] P. Korcyl and G. S. Bali, *Non-perturbative determination of improvement coefficients using coordinate space correlators in $N_f = 2 + 1$ lattice QCD*, *Phys. Rev.* **D95** (2017) 014505, [[1607.07090](#)].

- [31] M. Dalla Brida and S. Sint, *A dynamical study of the chirally rotated Schrödinger functional in QCD*, in *Proceedings, 32nd International Symposium on Lattice Field Theory (Lattice 2014): Brookhaven, NY, USA, June 23-28, 2014*, vol. LATTICE2014, p. 280, 2014. [1412.8022](#).
- [32] J. Heitger, F. Joswig, A. Vladikas and C. Wittemeier, *Non-perturbative determination of c_V , Z_V and Z_S/Z_P in $N_f = 3$ lattice QCD*, in *Proceedings, 35th International Symposium on Lattice Field Theory (Lattice 2017): Granada, Spain, June 18-24, 2017*, vol. 175, p. 10004, 2018. [1711.03924](#). [[doi:10.1051/epjconf/201817510004](#)].
- [33] M. Dalla Brida, T. Korzec, S. Sint and P. Vilaseca, “High precision renormalization of the non-singlet axial and vector currents in lattice QCD with Wilson quarks.” in preparation.